Time-Resolved Two-Pulse Excitation of Quantum Dots Coupled to a Photonic Crystal Cavity in the Purcell Regime

Jieun Lee, Timothy W. Saucer, Andrew J. Martin, Joanna M. Millunchick, and Vanessa Sih

Phys. Rev. Lett. **110**, 013602 — Published 4 January 2013

DOI: 10.1103/PhysRevLett.110.013602

Time-resolved two-pulse excitation of quantum dots coupled to a photonic crystal cavity in the Purcell regime

Jieun Lee,[1] Timothy W. Saucer,[1] Andrew J. Martin,[2] Joanna M. Millunchick,[2] and Vanessa Sih[1]

[1] *Department of Physics, University of Michigan, Ann Arbor, Michigan 48109, United States*
[2] *Department of Materials Science and Engineering, University of Michigan, Ann Arbor, Michigan 48109, United States*

(Dated: November 28, 2012)

We investigate the nonlinear emission dynamics of quantum dots coupled to photonic crystal cavities in the Purcell regime using luminescence intensity autocorrelation. Two laser pulses with a controlled time delay sequentially excite the coupled system inducing emission that depends on the delay and laser power. We find distinct contrasts between exciton and biexciton emission as a function of time delay which originate from different nonlinearities. A quantum optical simulation is also performed that accounts for the interaction between the laser pulses, exciton and cavity mode.

PACS numbers: 42.50.-p, 42.65.-k, 78.67.Hc

In the field of cavity quantum electrodynamics (QED), tailoring the optical environment of a quantum emitter can lead to the modification of spontaneous emission as first discovered by Purcell [1] and demonstrated in atoms [2] and solid-state systems [3–5]. The ability to modify the temporal and spectral features of quantum emitters using cavity QED is expected to greatly enhance the performance of optoelectronic devices such as quantum gates and micro-lasers. It has been recognized that for these applications utilizing the nonlinear optical response of cavity-coupled quantum emitters is advantageous [6–8]. For example, recent experiments have shown the ultrafast switching of two weak laser pulses enabled by the nonlinear response of a strongly coupled solid-state system [9, 10]. Earlier measurements in the weak coupling regime have also revealed complex nonlinear coupling dynamics [11].

Despite the importance of nonlinearity in cavity QED for both strong and weak coupling regimes, the effects of nonlinearity in modifying the temporal dynamics and quantum yield of coupled systems are not fully understood. In this work, we use luminescence intensity autocorrelation (LIA) to experimentally and theoretically investigate the dynamics of single emitters whose emission are enhanced by the Purcell effect, at various power regimes. This approach enables the direct visualization of the nonlinear emission as a function of time under constant incident power.

LIA is a time-resolved optical measurement that monitors the emission as a function of the delay time between two optical excitation pulses. Therefore both the power-dependent and time-resolved response of the excitation and emission can be simultaneously studied, with the temporal resolution limited only by the duration of the laser pulse. For LIA, the radiative lifetime of an emitter is measured through the nonlinear response of the time-averaged emission intensity, which is inherently different from time-resolved photo-detection methods using streak cameras [12] or photon correlation measurements [13].

Here we present a study on the nonlinear dynamics of single quantum dots (QDs) coupled to photonic crystal (PhC) cavities. The Purcell effect by the cavity is demonstrated by performing LIA on QDs both coupled and uncoupled to a cavity. The enhanced spontaneous emission of the cavity-coupled QDs enables a strong LIA signal which evolves when varying the incident power over a wide range. We also observe distinct differences between exciton and biexciton LIA, demonstrating the potential of LIA as a tool to identify the QD transitions.

For sample fabrication, 2.3 monolayers of InAs were deposited for QD nucleation and subsequently annealed at the growth temperature in order to blue-shift the emission wavelength [14]. Under these growth conditions, QDs nucleate with a density of $500/\mu\text{m}^2$ as verified by atomic force microscopy of an uncapped sample. For PhC fabrication, QDs are grown in the middle of a 150 nm GaAs layer which forms the membrane of the PhC. The final L3 cavity looks similar to the SEM image in Fig. 1(b).

The optical characterization of the QDs coupled to the PhC cavity is carried out using a HeNe laser. For the time-resolved experiment, pulses from a modelocked picosecond Ti:S laser (76 MHz repetition rate) tuned to a center wavelength of 780 nm with controlled time delay are used as the excitation source. An objective lens with numerical aperture NA = 0.7 and a fast-steering mirror controlling the beam path going to the sample are used to focus the beam on the cavity with 5 μm beam diameter. The emitted light from the sample is collected by the same objective lens and spatially resolved by a translational confocal microscopy configuration with a pinhole used as an aperture to selectively collect emission from QDs coupled to the cavity [15]. The collected light is recorded by a CCD detector with 1 s exposure time. The sample temperature was set to 10 K by a Helium-flow cryostat for all measurements.

The coupling between the PhC cavity and QDs are studied by polarization-dependent micro-

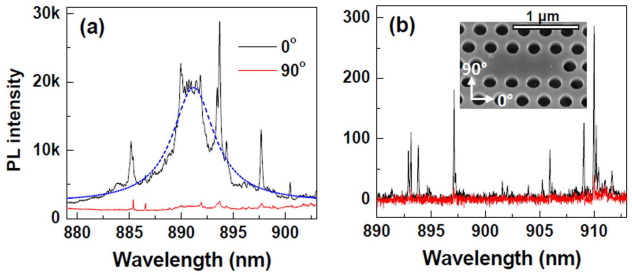

FIG. 1. (Color online) Purcell enhancement of PL from QDs embedded in a PhC cavity. The HeNe laser polarization was set to 45° relative to the cavity and the PL was collected at either 0 or 90° by using a half-wave plate ($\lambda/2$) and a polarizing beam splitter (PBS) as shown in Fig. 2(a). (a) PL spectra measured at a laser power = 190 μW. Blue dashed line is the Lorentzian fit. (b) PL spectra measured when laser power = 0.28 μW. Inset: SEM image of the L3 cavity. This image is tilted by 20°. The arrows show the orientation of the collected PL.

photoluminescence (PL) measurements as shown in Fig. 1. PL from QDs with emission wavelength well within the cavity mode are Purcell enhanced only when the PL polarization is parallel to the cavity mode field direction which is at 0° in this cavity [16]. From the Lorentzian fit of the Purcell enhanced PL at a laser power = 190 μW, the calculated cavity Q = 190 which corresponds to the cavity loss rate κ = 5500 GHz. At a lower laser power = 0.28 μW, a smaller number of Purcell enhanced QD emissions are observed. For both powers, the 90° polarized light emission is suppressed due to the polarization mismatch to the cavity mode [5].

In order to evaluate the Purcell enhancement by the cavity, we then directly measure the lifetime of the QDs using LIA. For the time-resolved experiment, two Ti:S pulses arrive at the sample with a relative time delay τ_d which is controlled by a mechanical delay line on one arm of the laser path [Fig. 2(a)]. To verify that the position of the delay line has minimal effect on the optical alignment, we first measured the PL when scanning the delay line and with the beam going to the other (fixed) path blocked. With the blocked fixed line, the 2D plot of the PL from three QDs coupled to the cavity while scanning the delay line is shown in Fig. 2(b). For every measurement, the variation in PL intensity for a delay line scan with the fixed path blocked was maintained to be below 5 %.

We then performed the time-resolved experiment with pulses from both the delay line and fixed arms on the same QDs [Fig. 2(c)]. For a long delay between pulses (> 1.5 ns), the PL intensity becomes about twice that of a single pulse, but when the two pulses are overlapped around zero time delay, the PL decreases. Such delay time dependence is observed in several QDs for the selected laser power (= 36 μW). The appearance of the dip at this laser power is related to the radiative recombination time (τ) of the QD. The origin of the dip will be examined in more detail with the simulation described below. Fitting the data to the exponential decay function $I = I_0 - I_1\exp(-\tau_d/\tau)$, for the QD with λ = 897.7 nm, we found τ = 0.5 ns [Fig. 2(e), black filled circles]. The autocorrelation function of the laser pulse is also plotted for reference.

To compare the lifetime of the Purcell enhanced QD to a QD without a cavity, we also measured LIA for a single QD with a similar emission wavelength in a different sample which has no cavity [Fig. 2(e), grey open circles], and the measured τ = 1 ns, similar to lifetimes of previously reported InAs QDs. Therefore the extracted Purcell factor F = 2 for this selected QD. The largest F we observed in this cavity is 4, corresponding to a measured τ = 0.25 ns. The variation of the measured Purcell factor from QDs is due to the different spatial and spectral match to

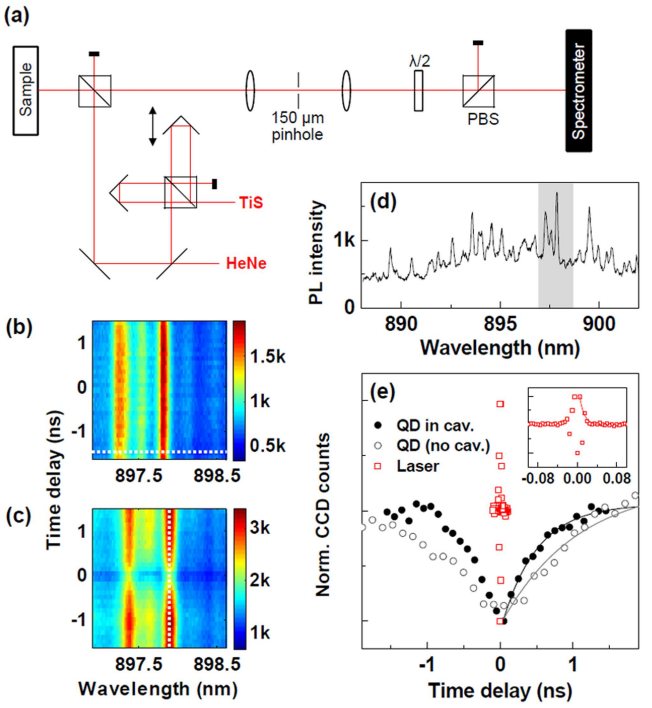

FIG. 2. (Color online) Experimental set-up and measured PL data. (a) Set-up. (b) The measured 2D plot shows the PL intensity of three QDs while varying the delay line position with the fixed line blocked. The measured spectrum at a delay line position (horizontal white line) is shown in the shaded area of (d). (c) The PL intensity with both arms unblocked exhibits a dependence on time delay. (e) For comparison of time-resolved data between QDs and laser autocorrelation, the detector CCD counts at large time delays are normalized. The black filled circles are measured from a cavity-enhanced QD and correspond to the vertical white line in (c). The grey open circles are from a QD that is not in a cavity. The inset shows the extended view of the laser autocorrelation (red open squares). The time-resolved data of both QDs and the laser are fitted to the exponential decay function.

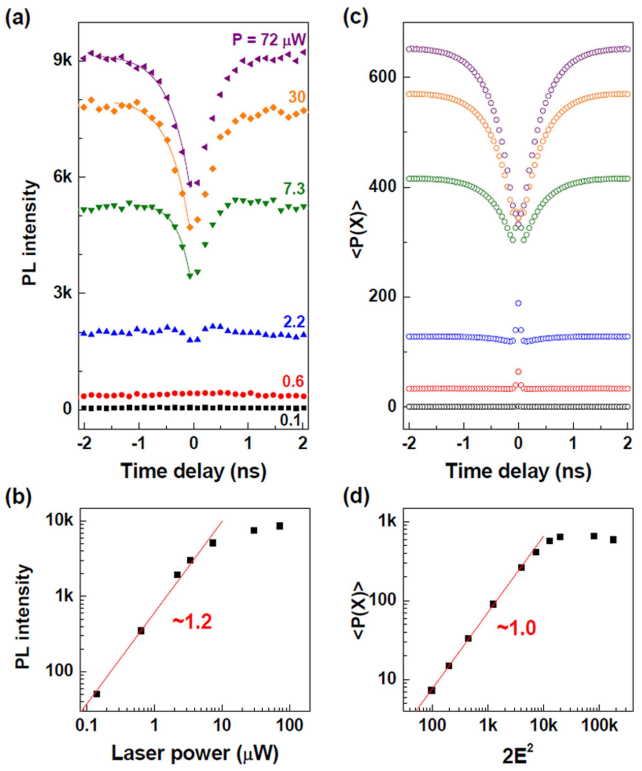

FIG. 3. (Color online) Power-dependent LIA of an exciton from both experiment (a),(b) and simulation (c),(d). (b) In the experiment, the linear power-dependence before the PL saturation shows that the peak is from an exciton. (a) From bottom to top, laser power increases. At the laser power where the QD nonlinearity appears, the dip starts to evolve in the time-resolved LIA. Similar results are obtained in the simulation (c).

the cavity mode [5].

We studied LIA in more detail by varying the laser power. Fig. 3(a) shows the experimentally measured PL intensity of a QD exciton as a function of time delay where the laser power increases from 0.1 to 71.9 μW. The laser power where the dip starts to appear is near where the QD emission saturates. This indicates that the evolution of LIA by varying the laser power results from the QD nonlinearity. Such QD nonlinearity is due to an atom-like quantized energy state of a single QD. It should be noted that this clear relation between the QD power dependence and LIA was not observed for an ensemble of QDs [17].

To understand the origin of the dip at high laser power where the QD emission saturates, let us consider the two cases where (i) $\tau_d = 0$ and (ii) $\tau_d >> \tau$. We are interested in a laser power where a single laser pulse can completely fill the QD exciton state. At $\tau_d = 0$, two laser pulses arrive at the QD simultaneously but they can fill the QD exciton state once. However, when $\tau_d >> \tau$, the first and the second pulse can each independently fill the QD since the exciton excited by the first pulse has enough time to relax before the second pulse arrives. Therefore we expect that the number of excitons generated when $\tau_d = 0$ to be half of when $\tau_d >> \tau$. In the experimental data, the ratios PL($\tau_d = 0$) / PL($\tau_d >> \tau$) of the 3 highest powers are $\{0.68, 0.64, 0.63\}$ for P = $\{7.3, 29.7, 71.9\}$ μW. As the laser power increases, the ratio approaches the expected value of 0.5. We consider that the experimentally observed ratio is higher than 0.5 due to imperfect alignment and a finite time step $\Delta\tau_d$ (= 0.13 ns).

The lifetime τ obtained from the 3 highest powers are $\{0.24, 0.38, 0.39\}$ ns for P = $\{7.3, 29.7, 71.9\}$ μW. Here the QD lifetime is increasing with laser power and saturating at some point. Note that the increase and saturation of τ with power was also observed on several QDs in a different cavity [Fig. 4]. The increase of τ, together with the decrease of the ratio PL($\tau_d = 0$) / PL($\tau_d >> \tau$), at the intermediate power range is the result of the partial state filling (< 100%) of the exciton state in the QD by the first pulse.

We also observed that the higher Q (= 680) of the cavity in Fig. 4 has reduced the laser power required for the onset of nonlinearity as compared to the cavity (Q = 190) shown in Fig. 3. This observation implies that nonlinearity at the single photon level is possible by increasing Q. Progress in this direction was recently made by the demonstration of nonlinearity with a few incident photons on a strongly coupled QD-pillar cavity device [18]. Another possible observation through LIA is the coherent dynamics (ex. Rabi oscillation) in the time domain.

In order to model the experimental data, we have conducted a simulation using the quantum optics toolbox [19]. In the simulation, we first constructed the Jaynes-Cummings Hamiltonian that takes into account the interaction between the two-level system and the cavity photon mode. The QD transition and cavity mode are assumed to be degenerate, similar to the selected experimental data. The pulsed laser is introduced as two Gaussian functions (width = 10 ps) with a time delay. Here

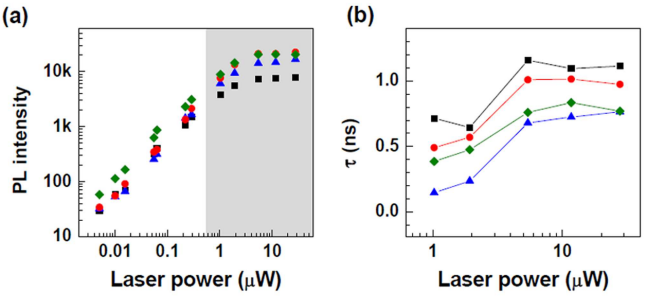

FIG. 4. (Color online) (a) PL intensity and (b) extracted exciton lifetime of four different QDs in a different cavity (Q = 680) as a function of laser power. Lifetimes are measured for the nonlinear power range (shaded area).

the energy of the laser is assumed to be resonant with the QD and the cavity, which is reasonable because any coherent effects due to the laser in the simulation cannot last longer than the pulse width (10 ps) which is much shorter than τ and the timescale of the dynamics that we are interested in. The dissipation factors are phenomenologically included in the Lindblad form for all calculations: $\kappa = 5500$ GHz, $\gamma = 1$ GHz, $\gamma_d = 40$ GHz. Here κ, γ, and γ_d are the cavity loss rate, QD transition rate, and the QD dephasing rate, respectively. κ and γ_d are from the measured cavity and QD emission width and γ is from the measured τ of the cavity-uncoupled QD. The dot-cavity coupling strength g is obtained by finding a best fit and the resultant g = 42 GHz. From these parameters, the calculated critical photon number $n_0 = 0.01$ which is well below one. The critical photon number is a measure of the number of photons required in the cavity mode in order to saturate the QD [20]. Therefore any photon number N above n_0 could be used to include the power nonlinearity in the simulation. In our calculation, using photon number $N = 1$ to 4 showed similar results. The single pulse amplitude E was varied to incorporate the varying laser power of the two pulses ($2E^2$). An alternative to this quantum optical simulation has also been reported which solves the nonlinear semiclassical model [21].

In our simulation, the average QD exciton state population <P(X)> was calculated for each E while varying the time delay between the two pulses. We find excellent similarity between the experimental data and the simulation [Fig. 3(a),(c)]. In addition, the dip in the simulation starts to appear at the power where <P(X)> saturates which is consistent with the experimental data. Using a single set of physical parameters, the lifetime τ of the simulation in the nonlinear regime is 0.38 ns for all E. The peak around zero time delay is the result of resonant excitation that could not be washed out in the simulation within the pulse overlap ($\tau_d < 20$ ps).

Finally, we show the experimental result of QD biexciton emission in Fig. 5. Due to the superlinear power dependence in the low power regime, the PL intensity at zero delay time is higher than the PL at large time delays. Such a rise at low power can be understood by the formation of a biexciton through the combination of two excitons, one from each of the first and the second laser pulse, which is possible only when the two pulses arrive within the lifetime of the exciton. Therefore the fitted τ at low laser power is related to the recombination time of both the exciton and biexciton [22]. At higher laser power, the sublinear power dependence results in a dip in the time-resolved data, similar to what we observe for exciton emission. At the lowest laser power, no features are observed due to the reduced probability of creating a biexciton. In our sample, due to the high density of QDs, the corresponding exciton peak of this biexciton was hard to identify. By isolating the emission from a single QD, direct comparison between the QD exciton and biexciton lifetime will be possible.

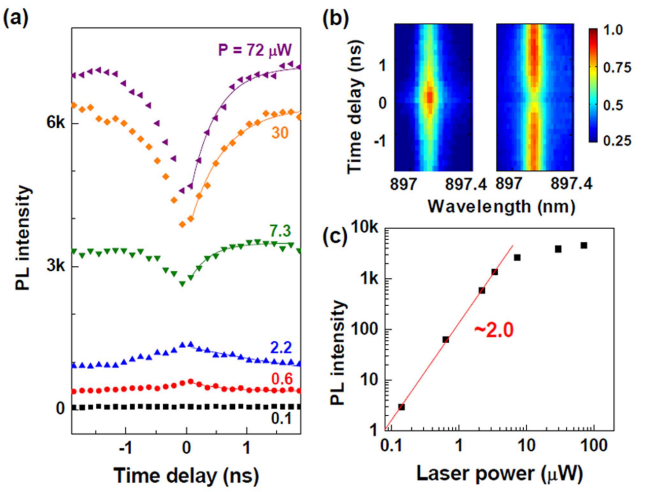

FIG. 5. (Color online) Power-dependent LIA of a biexciton. (a) Unlike the exciton, biexciton emission shows a rise at low laser powers. This is consistent with the superlinear power dependence of the biexciton emission (c). τ from an exponential fit from bottom to top are 0.6, 3.5, 0.33, 0.56, 0.44 ns (lowest laser power excluded). (b) The change from rise to dip is more apparent in the 2D plot (Left: P = 2.2 μW, Right: P = 7.3 μW). The color scales of both plots are normalized.

In conclusion, the nonlinear dynamics of a dot-cavity coupled system is studied by LIA, which is a power-dependent and time-resolved measurement method using two time-delayed degenerate laser pulses. Modeling the excitonic LIA using a quantum optical simulation, we found physical parameters governing the coupling (g) and emission dynamics (κ, γ) for a cavity-coupled QD in the Purcell regime. The LIA signal of the Purcell enhanced QD is negative (dip) for laser powers above the dot saturation point, which is qualitatively the same as the QD outside the cavity except that the dip is narrower due to the shorter lifetime. We expect that positive or even oscillating excitonic LIA can be observed by increasing Q to the strong coupling [9, 10] or lasing regime [11]. This method can be applied to study the nonlinear emission dynamics of various types of quantum structures for the next generation of quantum lasers and quantum information processing.

The authors would like to acknowledge Duncan G. Steel for helpful discussions. Sample fabrication was performed at the Lurie Nanofabrication Facility at the University of Michigan, part of the NSF funded NNIN network. This work was supported by the National Science Foundation Materials Research Science and Engineering Center program DMR 1120923.

[1] E. M. Purcell, Phys. Rev. **69**, 681 (1946).

[2] H. Walther, B. T. H. Varcoe, B.-G. Englert, and T. Becker, Rep. Prog. Phys. **69**, 1325 (2006).

[3] A. Kiraz, P. Michler, C. Becher, B. Gayral, A. Imamoğlu, L. Zhang, E. Hu, W. V. Schoenfeld, and P. M. Petroff, Appl. Phys. Lett. **78**, 3932 (2001).

[4] P. Lodahl, A. F. V. Driel, I. S. Nikolaev, A. Irman, K. Overgaag, D. Vanmaekelbergh, and W. L. Vos, Nature **430**, 654 (2004).

[5] D. Englund, D. Fattal, E. Waks, G. Solomon, B. Zhang, T. Nakaoka, Y. Arakawa, Y. Yamamoto, and J. Vučković, Phys. Rev. Lett. **95**, 013904 (2005).

[6] S. Strauf, K. Hennessy, M. T. Rakher, Y.-S. Choi, A. Badolato, L. C. Andreani, E. L. Hu, P. M. Petroff, and D. Bouwmeester, Phys. Rev. Lett. **96**, 127404 (2006).

[7] K. Srinivasan and O. Painter, Nature **450**, 862 (2007).

[8] A. Auffèves-Garnier, C. Simon, J.-M. Gérard, and J.-P. Poizat, Phys. Rev. A **75**, 053823 (2007).

[9] D. Englund, A. Majumdar, M. Bajcsy, A. Faraon, P. Petroff, and J. Vučković, Phys. Rev. Lett. **108**, 093604 (2012).

[10] R. Bose, D. Sridharan, H. Kim, G. S. Solomon, and E. Waks, Phys. Rev. Lett. **108**, 227402 (2012).

[11] D. K. Young, L. Zhang, D. D. Awschalom, and E. L. Hu, Phys. Rev. B **66**, 081307(R) (2002).

[12] A. Laucht, M. Kaniber, A. Mohtashami, N. Hauke, M. Bichler, and J. J. Finley, Phys. Rev. B **81**, 241302(R) (2010).

[13] M. Winger, T. Volz, G. Tarel, S. Portolan, A. Badolato, K. J. Hennessy, E. L. Hu, A. Beveratos, J. Finley, V. Savona, and A. Imamoğlu, Phys. Rev. Lett. **103**, 207403 (2009).

[14] B. D. Gerardot, G. Subramanian, S. Minvielle, H. Lee, J. A. Johnson, W. V. Schoenfeld, D. Pine, J. S. Speck, and P. M. Petroff, J. Cryst. Growth **236**, 647 (2002).

[15] J. Lee, T. W. Saucer, A. J. Martin, D. Tien, J. M. Millunchick, and V. Sih, Nano Lett. **11**, 1040 (2011).

[16] J. D. Joannopoulos, S. G. Johnson, J. N. Winn, and R. D. Meade, *Photonic Crystals: Molding the Flow of Light* (Princeton University Press, Princeton, 2008).

[17] L.-C. Su, D.-C. Wu, and M.-H. Mao, IEEE Photon. Technol. Lett. **21**, 289 (2009).

[18] V. Loo, C. Arnold, O. Gazzano, A. Lemaître, I. Sagnes, O. Krebs, P. Voisin, P. Senellart, and L. Lanco, Phys. Rev. Lett. **109**, 166809 (2012).

[19] S. M. Tan, J. Opt. B: Quantum Semiclass. Opt. **1**, 424 (1999).

[20] H. J. Kimble, Phys. Scripta **T76**, 127 (1998).

[21] A. Majumdar, D. Englund, M. Bajcsy, and J. Vučković, Phys. Rev. A **85**, 033802 (2012).

[22] G. Bacher, R. Weigand, J. Seufert, V. Kulakovskii, N. A. Gippius, A. Forchel, K. Leonardi, and D. Hommel, Phys. Rev. Lett. **83**, 4417 (1999).